Functional Nanoparticles Activate a Decellularized Liver Scaffold for Blood Detoxification

Fen Xu, Tianyi Kang, Jie Deng, Junli Liu, Xiaolei Chen, Yuan Wang, Liang Ouyang, Ting Du, Hong Tang, Xiaoping Xu, Shaochen Chen, Yanan Du, Yujun Shi, Zhiyong Qian, Yuquan Wei, Hongxin Deng,* and Maling Gou*

Extracorporeal devices have great promise for cleansing the body of virulence factors that are caused by venomous injuries, bacterial infections, and biological weaponry. The clinically used extracorporeal devices, such as artificial liver-support systems that are mainly based on dialysis or electrostatic interaction, are limited to remove a target toxin. Here, a liver-mimetic device is shown that consists of decellularized liver scaffold (DLS) populated with polydiacetylene (PDA) nanoparticles. DLS has the gross shape and 3D architecture of a liver, and the PDA nanoparticles selectively capture and neutralize the pore-forming toxins (PFTs). This device can efficiently and target-orientedly remove PFTs in human blood ex vivo without changing blood components or activating complement factors, showing potential application in antidotal therapy. This work provides a proof-of-principle for blood detoxification by a nanoparticle-activated DLS, and can lead to the development of future medical devices for antidotal therapy.

1. Introduction

Extracorporeal detoxification devices offer clinical ways to cleanse the blood of virulence factors.[1–3] Pore-forming toxins (PFTs), one of the most common protein toxins in nature, underlie the virulence mechanisms in animal bites/sting and bacterial infections,[4–8] Over 80 families of PFTs have been identified, displaying diverse molecular structures,

Dr. F. Xu, Dr. T. Kang, Dr. J. Deng, Dr. J. Liu, Dr. X. Chen, Y. Wang,
Dr. L. Ouyang, T. Du, Prof. Z. Qian, Prof. Y. Wei, Prof. H. Deng, Prof. M. Gou
State Key Laboratory of Biotherapy and Cancer Center
West China Hospital
Sichuan University
and Collaborative Innovation Center for Biotherapy
Chengdu 610041, China
E-mail: denghongx@scu.edu.cn; goumaling@scu.edu.cn

Dr. F. Xu
State Key Laboratory of Cardiovascular Disease
Fuwai Hospital
National Center for Cardiovascular Disease
Chinese Academy of Medical Sciences and Peking
Union Medical College
Beijing 100037, China

Prof. H. Tang
Center of Infectious Diseases
West China Hospital
Sichuan University
Chengdu 610041, China

Prof. X. Xu
West China School of Pharmacy
Sichuan University
Chengdu 610041, P. R. China

Prof. S. Chen
Department of NanoEngineering
University of California
San Diego, CA 92093, USA

Prof. Y. Du
Department of Biomedical Engineering
School of Medicine
Tsinghua University
Beijing 100084, China

Prof. Y. Shi
Laboratory of Pathology
West China Hospital
Sichuan University
Key Laboratory of Transplant Engineering and Immunology
NHFPC, West China Hospital
Sichuan University
Chengdu 610041, China

different molecular weight, and distinctive epitopic targets.[9] Currently, there is no clinical detoxification device that can targetedly remove PFTs from blood, despite the existed liver-support systems which remove toxins by dialysis or ionic adsorption column can benefit patients who suffer from PFTs.

Nanoparticles can be rationally designed to bind and neutralize target toxins, owing to their inherent small size and flexibility in design and preparation.[10–15] All PFTs have the same capacity to disrupt cells by forming pores in cellular membranes and altering their permeability. Recent advancements have spurred the development of an action mechanism-targeted detoxification of PFTs by nanoparticles that function as a toxin decoy to attract and trap PFTs, which allows one nanoparticle to capture and neutralize different PFTs.[16,17] Therefore, a fluidic system that is integrated with retrievable nanoparticles has potential application in PFTs detoxification by targetedly removing PFTs from the bloodstream.

The liver is an important apparatus of our body which has the function of detox, in which the liver-specific microstructure facilitates hepatocytes to efficiently detoxify the bloodstream.[18,19] This inspired the design of a liver-mimetic fluidic device for detoxification. And it is of great interest to integrate nanoparticles into a liver-like fluidic systems for the efficient removal of toxins. Herein, we performed an attempt to use polydiacetylene (PDA) nanoparticles to "recellularize" an animal decellularized liver scaffold (DLS), to construct a liver-mimetic device for human blood detoxification. PDA nanoparticles were derived from self-assembly of 10,12-pentacosadiynoic acid (PCDA). The nanoparticle surface is made of a microvasculature π-conjugated polymer with alternating double- and triple-bond groups in the main polymer chain. The cell membrane-mimic surface functions to attract, capture, and neutralize toxins owing to the interactions between PDA and PFTs.[2] DLS preserves the gross shape and 3D architecture of a liver which is a naturally precise microfluidic system. Our results indicate that the liver-mimetic device (named as PDA-DLS device) can efficiently remove PFTs toxins in human blood ex vivo, and does not affect blood components and complement factors. This work might inspire many breakthroughs in the development of extracorporeal device that can efficiently remove target toxins from bloodstream for future clinical use.

2. Results

### 2.1. Preparation of a Nanoparticle-Activated Liver-Mimetic Device

The PDA-DLS device is schematically presented in **Figure 1**. To generate this device, we used a decellularization technology to prepare the DLS, followed by seeding with PDA nanoparticles. By portal vein perfusion with sodium dodecyl sulfate (SDS), a rat liver was gradually decellularized, and became a translucent DLS with the gross shape of liver (**Figure 2**A). Hematoxylin-eosin staining and immunostaining indicated that DLS without cells preserves similar structural

✳ Toxins   🔴 Blood cells   🔵 Nanoparticles
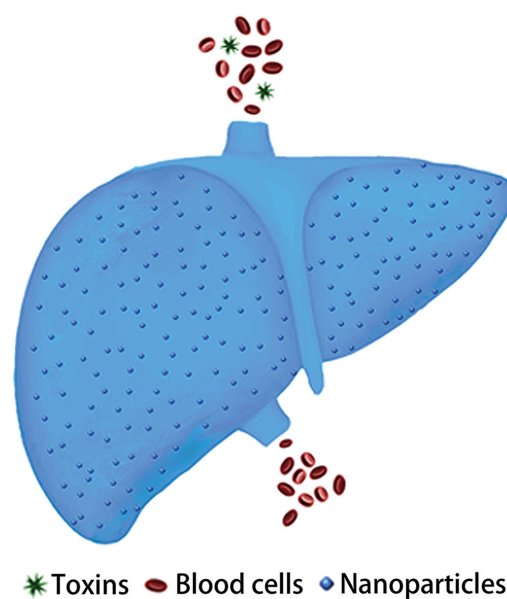
Figure 1. Schematic presentation of the liver-mimetic device that consists of DLS populated with PDA nanoparticles. This device is designed to remove toxins in bloodstream.

and basic membrane components of the extracellular matrix proteins to native liver (Figure 2B). The residual DNA and cellular protein in DLS were not detected (**Figure 3**A,B). DLS maintained the liver's 3D collagenous fibers network intact (Figure 3C,D). After trypan blue as a dye was injected through the portal vein, it gradually moved from larger vessels to smaller capillaries, suggesting the presence of an intact microvasculature in DLS (Figure 3E,F). The corrosion cast of DLS showed a portal and venous circulation system of vessels with microcirculatory branches, which implied that the blood flow could be achieved by traversing the portal venous system and emptying into the systemic venous circulation via the hepatic vein and inferior vena cava (IVC) (Figure 3G). It was also directly observed that the large vessel and small vessels closely resembling portal triad in DLS by scanning electron microscope (SEM) (Figure 3H,I). Therefore, the decellularization process selectively removed the cellular components of the liver and preserved the extracellular matrix components as well as the intact vascular network in DLS.

After the DLS was obtained, it was populated with PDA nanoparticles as artificial cells. The PDA nanoparticles were modified to possess the leaving group N-hydroxysuccinimide (NHS) on its surface which can interact with the amino group of collagen (**Figure 4**A,B). Thus, the PDA nanoparticle could be chemically tethered to the collagenous fibers of DLS by the amide group (schematically presented in Figure 4C). The resultant PDA nanoparticles have a mean particle size of ≈100 nm (Figure 4D) and a zeta potential of −20 mV (Figure 4E). Under transmission electron microscopy, this nanoparticle exhibited a vesicle structure approximately 80 nm in diameter (Figure 4F). PDA nanoparticles with a light blue color were pumped into DLS through the portal vein to activate DLS. The outflow from IVC was clear, implying that the PDA nanoparticles were completely detained in DLS.
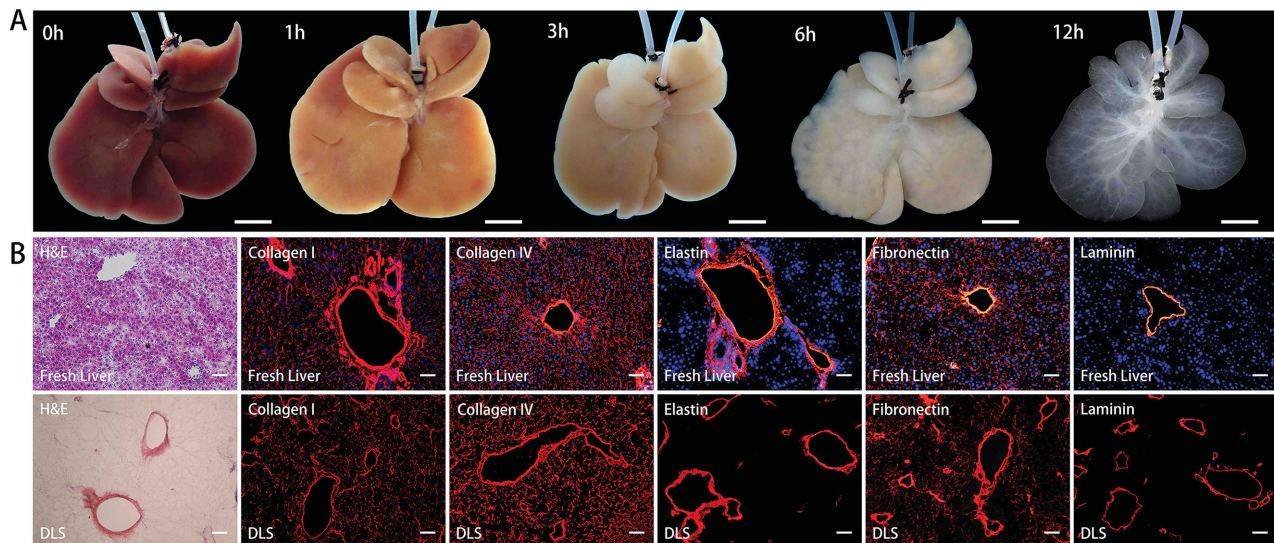
Figure 2. Decellularization of rat liver. A) Representative images of a fresh liver during the decellularization process at 0 h, 1 h, 3 h, 6 h, and 12h. B) Comparison of the fresh liver (top) and DLS (bottom). Left to right: H&E, collagen I (red), collagen IV (red), elastin (red), fibronectin (red), and laminin (red) staining. Sections were counterstained with DAPI (blue). Scale bars: 10 mm (A), 100 μm (B).

It was also observed that unmodified PDA nanoparticles could not be efficiently trapped in the DLS (Supplementary video, Supporting Information). Furthermore, the colorimetric readings of the outflows indicated that 100% PDA nanoparticles were detained in DLS (**Figure 5**A). Thus, the chemical modification of PDA nanoparticles is necessary for efficiently immobilizing PDA nanoparticles into DLS. Furthermore, when PDA-DLS was eluted with distilled water or human fresh blood, the immobilized PDA nanoparticles would not be released (Figure 5 B, C). By perfusion of DLS with 50 mg of PDA nanoparticles, a PDA-DLS device was created. The appearance of this device was shown in Figure 5D. Under transmission electron microscopy, it was observed that PDA nanoparticles were tethered to the surface of collagenous fibers within the PDA-DLS device (Figure 5E).

## 2.2. Removal of PFTs in Solution In Vitro

The ability of the PDA-DLS device to detoxify PFTs was tested by red blood cells (RBC) lysis test. Melittin was used as the model PFT. The capacity of the PDA-DLS device in detoxifying the melittin solution was compared with that of the fresh liver. The PDA-DLS device and the fresh liver (as control) were processed into pieces with the volume of 100 mm³, respectively, followed by incubation of each piece with melittin solutions (200 μL) of different concentrations. After incubation for 60 min, the samples were centrifuged, and the supernatants were added to rat RBC solution undergoing RBC lysis test. The centrifuged RBC solution in each test was shown in **Figure 6**A. The red color of the supernatant means hemolysis. And the PDA-DLS device was more efficient in detoxifying melittin than that of the fresh liver.
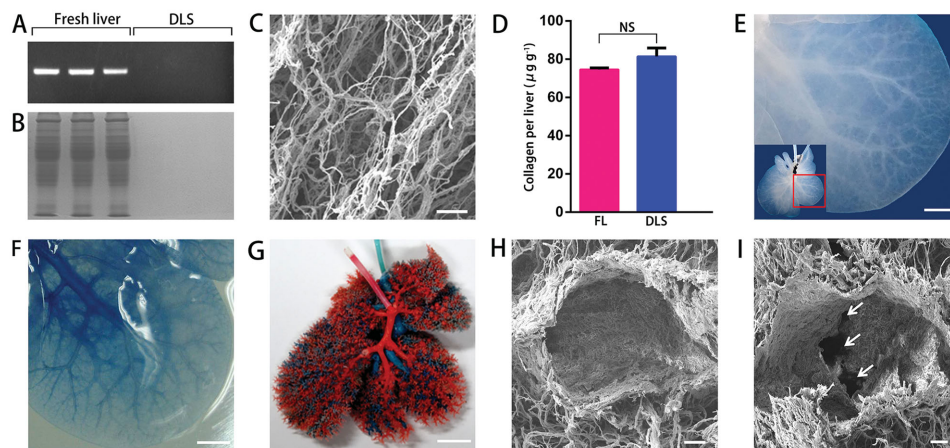
Figure 3. DLS retains intact collagen structure and vascular bed except for cells. A,B) Genomic DNA (A) and cellular protein (B) in the fresh liver (FL) and DLS. C) Scanning electron microscope image (SEM) of the collagenous fibers in DLS. D) Biochemical quantification of total collagen in FL and DLS. NS: no significant difference. E) Representative image of median lobe of DLS with the visible vascular tree. F) The vascular tree of median lobe after perfusion with trypan blue. G) Corrosion cast model of DLS with portal (red) and venous (blue) vasculature. H,I) Representative SEM images of a big vessel (H) and a section featuring portal tract (arrows) (I). Scale bars: 10 μm (C), 5 mm (E, F), 10 mm (G), 10 μm (H, I).
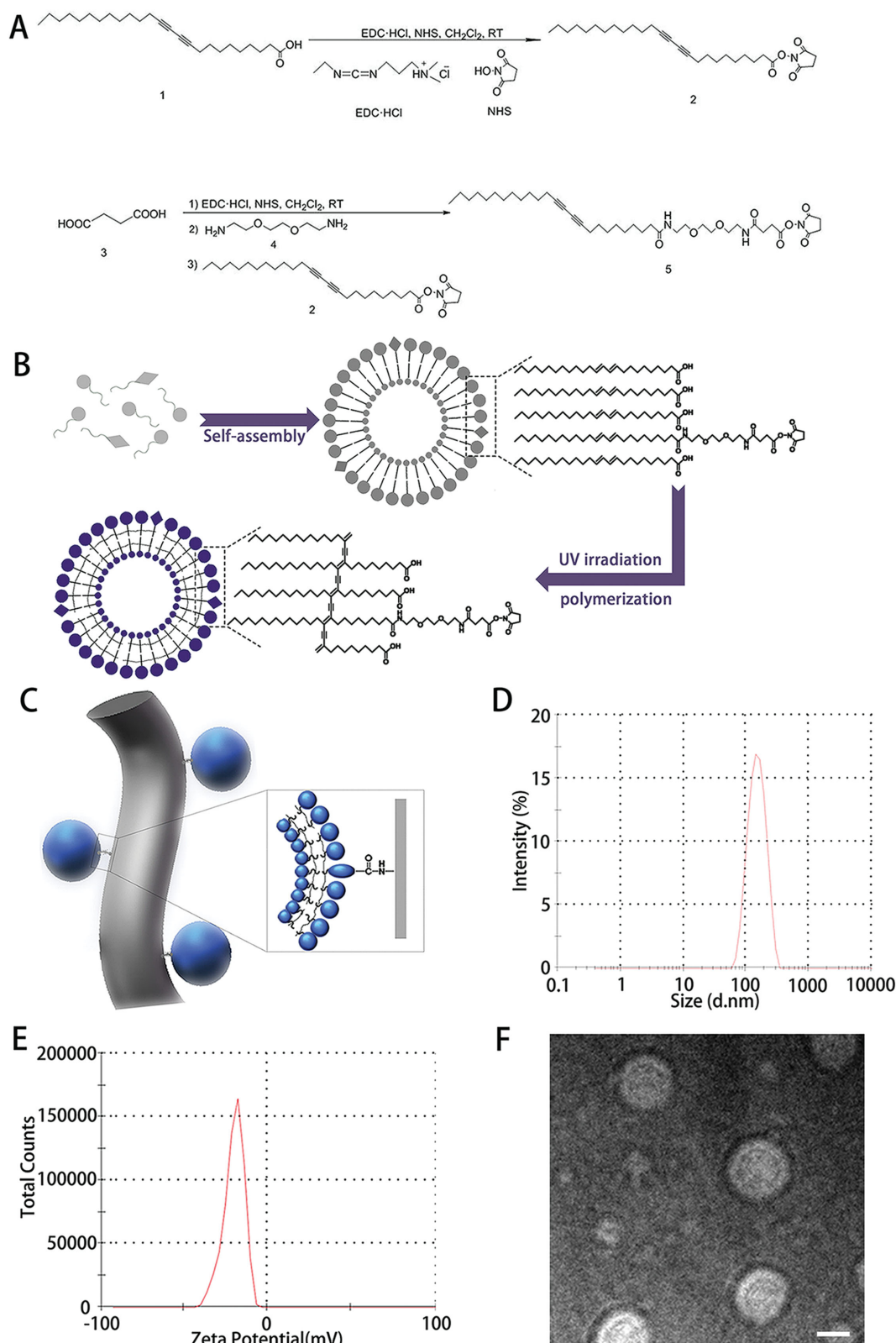
Figure 4. Preparation of PDA nanoparticles. A) Synthesis scheme of PCDA-EDEA- SA-NHS. B) Schematic presentation on the bilayer structure of PDA nanoparticles and how they are assembled. PCDA and PCDA-EDEA-SA-NHS were self-assembled into colorless nanoparticles after undergoing probe sonication at 70 °C. Polymerization of PCDA via a 1,4-addition reaction was achieved by UV irradiation at 254 nm, forming a blue polymer with alternating double-triple bond. C) Schematic presentation that PDA nanoparticles are chemically tethered to the collagenous fibers within DLS by amide group. D, E) Particle size and zeta potential of PDA nanoparticles. The particle size distribution spectrum (D). The zeta potential distribution spectrum (E). This data was determined by Malvern Nano-ZS Instrument. The test temperature was 25 °C. F) Transmission electron microscopy image of PDA nanoparticles. Scale bars: 50 nm (F).
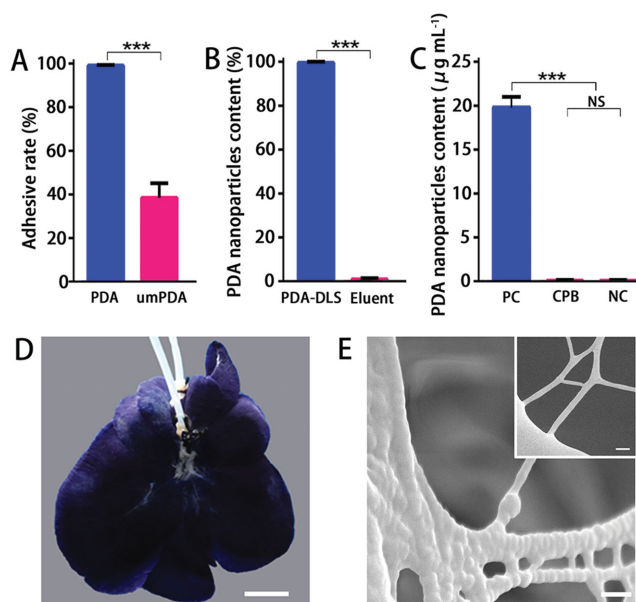
Figure 5. Immobilization of PDA nanoparticles in DLS. A) The efficiency of immobilizing PDA nanoparticles in DLS. umPDA: unmodified PDA nanoparticles. $n = 3$. B,C) The release of PDA nanoparticles from DLS. DLS reloaded with PDA nanoparticles was eluted with distilled water perfusion for 24 h. $n = 3$ (B). DLS reloaded with PDA nanoparticles was circularly perfused with human fresh blood for 20 min. $n = 3$ (C). PC (positive control): human fresh blood with 20 μg mL^{-1} PDA nanoparticles. CPB: circularly perfused human fresh blood. NC (negative control): human fresh blood. D) Representative images of the PDA-DLS device. The dark blue color of the device is owned to the population of blue PDA nanoparticles. E) SEM images of the PDA-DLS device and DLS (upper right). Scale bar: 10 mm (D), 200 nm (E).

Meanwhile, the detoxification efficiency was quantified via colorimetric readings. As presented in Figure 6B, the maximum concentration of melittin solution that the PDA-DLS device and the fresh liver could completely detoxify was 80 and 10 μg mL^{-1}, respectively. Therefore, the capacity of the PDA-DLS device in detoxifying melittin is about eight times stronger than that of the fresh liver. Furthermore, the efficiency of the PDA-DLS device in detoxifying the perfused melittin solution was evaluated. Melittin solution (10 μg mL^{-1}, 100 mL) was pumped into the PDA-DLS device or DLS (as control) through portal vein at 2 mL min^{-1}. Outflows were collected from IVC every 5 min, followed by RBC lysis tests. As presented in Figure 6C, the red supernatant means the residual of melittin in the outflow that could damage the cellular membrane. The color of supernatants suggested that the PDA-DLS device completely detoxified the sing-pass perfused melittin solution, while DLS alone did not significantly reduce the virulence of the perfused solution. The quantified detoxification efficiency was presented in Figure 6D. The efficiency of the PDA-DLS device in detoxifying a single-pass perfused melittin solution remains 100%, while the DLS's effect is negligible. This result implies that the ability of the PDA-DLS device in detoxification is mainly contributed by the PDA nanoparticles. Taking advantage of the fluorescence enhancement (none-to-fluorescence) of the PDA nanoparticles after binding toxins,[2] we detected the PDA-DLS device fluorescence that could reflect the capture

of toxins by nanoparticles. Under live fluorescence imaging, we observed that the PDA-DLS device displayed a none-to-red fluorescence change after perfusion with melittin solution, indicating the capture of melittin by PDA nanoparticles (as shown in Figure 6E). Meanwhile, in the confocal laser scanning microscope image, the PDA and melittin complex associated red fluorescence dot was directly observed. It was confirmed that the PDA nanoparticles were immobilized on the collagenous fibers as well as vascular walls (Figure 6F), and did not block the vessels (Figure 6G). Then, the PDA-DLS device was further used to detoxify circulating perfused solution to mimic detoxifying circulating blood by liver under physiological conditions. 100 mL melittin solution (10 μg mL^{-1}) was pumped into the PDA-DLS device through portal vein at 2 mL min^{-1}, and the outflow from IVC was collected in the melittin solution pool. The virulence of the melittin solution pool was examined by RBC lysis every 25 min. As shown in Figure 6H, the clear supernatant means no virulence of the melittin solution after circulating perfusion. It was observed that the PDA-DLS device could completely detoxify the circularly perfused melittin solution. The efficiency of detoxifying circularly perfused melittin solution was quantified, which indicated that the detoxification efficiency reached 100% after the melittin solution circulated for 75 min (1.5 times as much as that of single-pass perfusion) in our experimental condition (Figure 6I). These results demonstrate that the PDA-DLS device can efficiently detoxify the circulating perfusion solution.

2.3. Removal of PFTs in Human Blood Ex Vivo

To evaluate the efficiency of the PDA-DLS device in detoxifying melittin contaminated blood, the PDA-DLS device underwent circulating perfusion of human blood (20 mL) mixed with melittin (10 μg mL^{-1}). After circulation perfusion for 20 min (two times as much as that of single-pass perfusion), the detoxified blood was compared with fresh blood (Normal group) and melittin contaminated blood without any treatment (Melittin group). As shown in **Figure 7**A, the plasma in the PDA-DLS device group was clearer than that in Melittin group, suggesting that the PDA-DLS device treatment efficiently reduced the melittin-caused lysis of RBC. The RBC count study also indicated that the hemolysis rate of the PDA-DLS device group was obviously less than that of the Melittin group (Figure 7B). The total bilirubin and indirect bilirubin (two other positive correlation indexes of hemolysis) examination confirmed the lower hemolysis rate in the PDA-DLS device group (Figure 7C,D). Meanwhile, blood smears were prepared for observing the RBC morphology of each group. The normal RBC has a smooth donut-shape. Melittin changed the normal RBC into ancanthocytes which is closely associated with hemolysis. In the PDA-DLS device group, the proportion of ancanthocytes in RBC was much lower than that in Melittin group (Figure 7E). This implies that the PDA-DLS device can efficiently remove melittin from circulating blood and effectively protect RBC from damage by melittin.
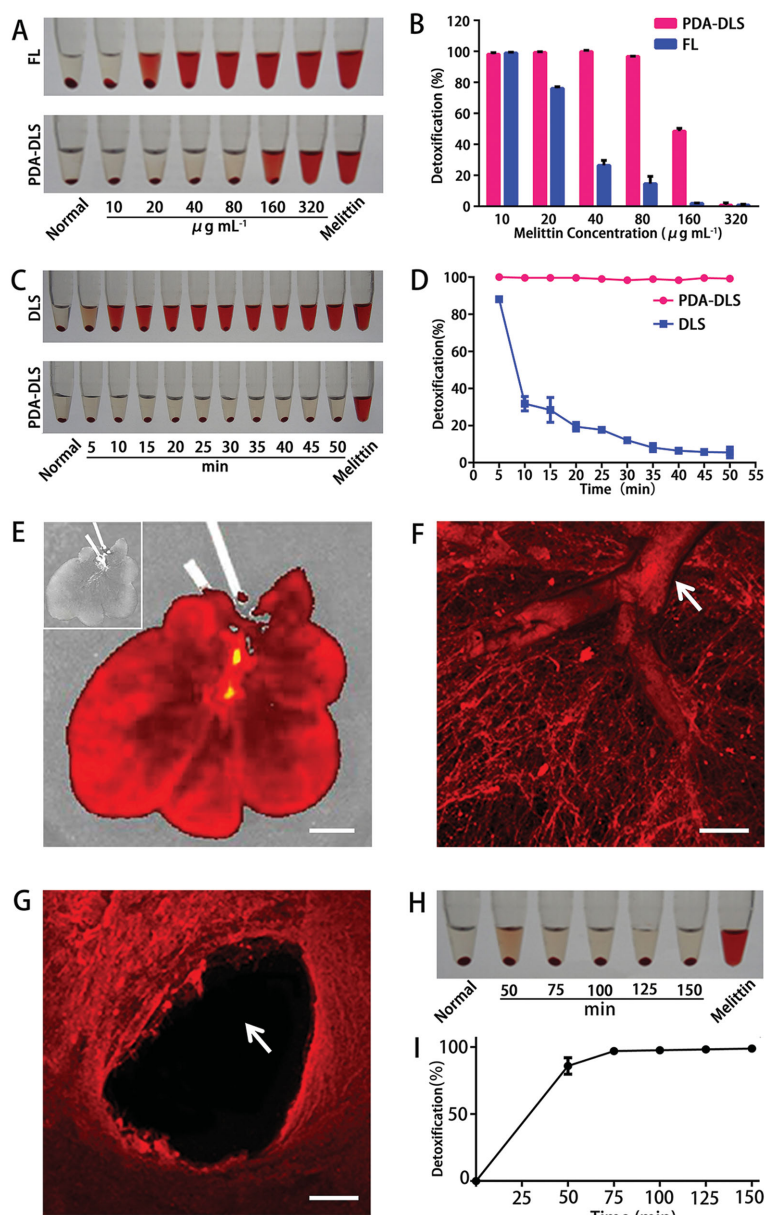
Figure 6. The capacity of PDA-DLS device in removing toxin in solution. A) Centrifuged RBC after incubation with melittin solution of different concentrations treated by 100 mm^3 of the fresh liver (FL) or the PDA-DLS device. The red color of the supernatant means hemolysis. Normal saline (Normal) and melittin solution (10 μg mL^{-1}, Melittin) were used as the negative control and positive control, respectively. B) Quantified efficiency of detoxifying the melittin solution with deferent concentration by 100 mm^3 of the fresh liver or the PDA-DLS device. $n = 3$. C) Centrifuged RBC after incubation with the melittin solution (10 μg mL^{-1}) that was treated by DLS or the PDA-DLS device via single-pass perfusion at different time points. Normal saline (Normal) and melittin solution (10 μg mL^{-1}, Melittin) were used as the negative control and positive control, respectively. D) Quantified efficiency of detoxifying a single-pass perfused melittin solution (10 μg mL^{-1}) by DLS or the PDA-DLS device. $n = 3$. E) Live fluorescent images of the whole PDA-DLS device before (upper left) and after (red) detoxifying the melittin solution (10 μg mL^{-1}, 100 mL).The red fluorescence is emitted by PDA and melittin complex. F,G) Representative confocal laser scanning microscopy images of the collagenous fibers and a big vessel (arrow) (F) and the section featuring of a vessel (arrow) (G) in the PDA-DLS device after detoxifying the melittin solution. The red fluorescence dot is PDA and melittin complex. H) Centrifuged RBC solution after incubation with melittin solution (10 μg mL^{-1}) treated by the PDA-DLS device via circulating perfusion at different time points. Normal saline (Normal) and melittin solution (10 μg mL^{-1}, Melittin) were used as the negative control and positive control, respectively. I) Quantified efficiency of detoxifying a circulating perfused melittin solution (10 μg mL^{-1}) treated by the PDA-DLS device. $n = 3$. Scale bar: 10 mm (E), 20 μm (F,G).

2.4. Safety Assessment of PDA-DLS Device

To evaluate the effect of the PDA-DLS device on normal human blood, the PDA-DLS device was circularly perfused with fresh human blood (100 mL) through the portal vein at 2 mL min^{-1} for 100 min. After perfusion, the blood cells maintained normal morphology (**Figure 8**A,B), and there was no significant change in the number of blood cells (Figure 8C–E). In addition, blood biochemical analysis showed that total protein and albumin of blood were not significantly reduced in the process of perfusion (Figure 8F,G). The impact of the PDA-DLA device on complement activation was compared with that of the fresh liver. After perfused through the fresh rat liver, the human blood suffered from a significant decrease of C3 and C4 and an increase in SC5b9, which implies that the complement in human blood was activated by heterogeneous fresh liver (Figure 8H–J). After treatment with the PDA-DLS device, the perfused human blood maintains similar content of C3, C4, and SC5b9 to that of the initial fresh blood (Figure 8H–J). Thus, applying the PDA-DLS device in blood detoxification would not significantly affect the quality of perfused normal blood.

3. Discussion

PDA is known as a sensor materials whose color (blue-to-red) and fluorescence (non-to-fluorescent) changes in response to environmental cues.[20–26] Because of the cellular membrane-mimetic surface and the conjugated structure, PDA nanoparticles promise the capacity in selectively capturing and neutralizing PFTs.[2] The direct intravenous administration of nanoparticles for antidotal therapy often leads to nanoparticle accumulation in the liver, posing a risk of secondary poisoning especially in liver-failure patients.[13,27] In this work, we used PDA nanoparticles to activate DLS, constructing anextracorporeal detoxification device that could efficiently and targetedly remove PFTs in circulating blood without affecting the blood components and complement factors. This indicated that the liver-mimetic device can remove PFTs in bloodstream, showing potential application in antidotal therapy against PFTs.
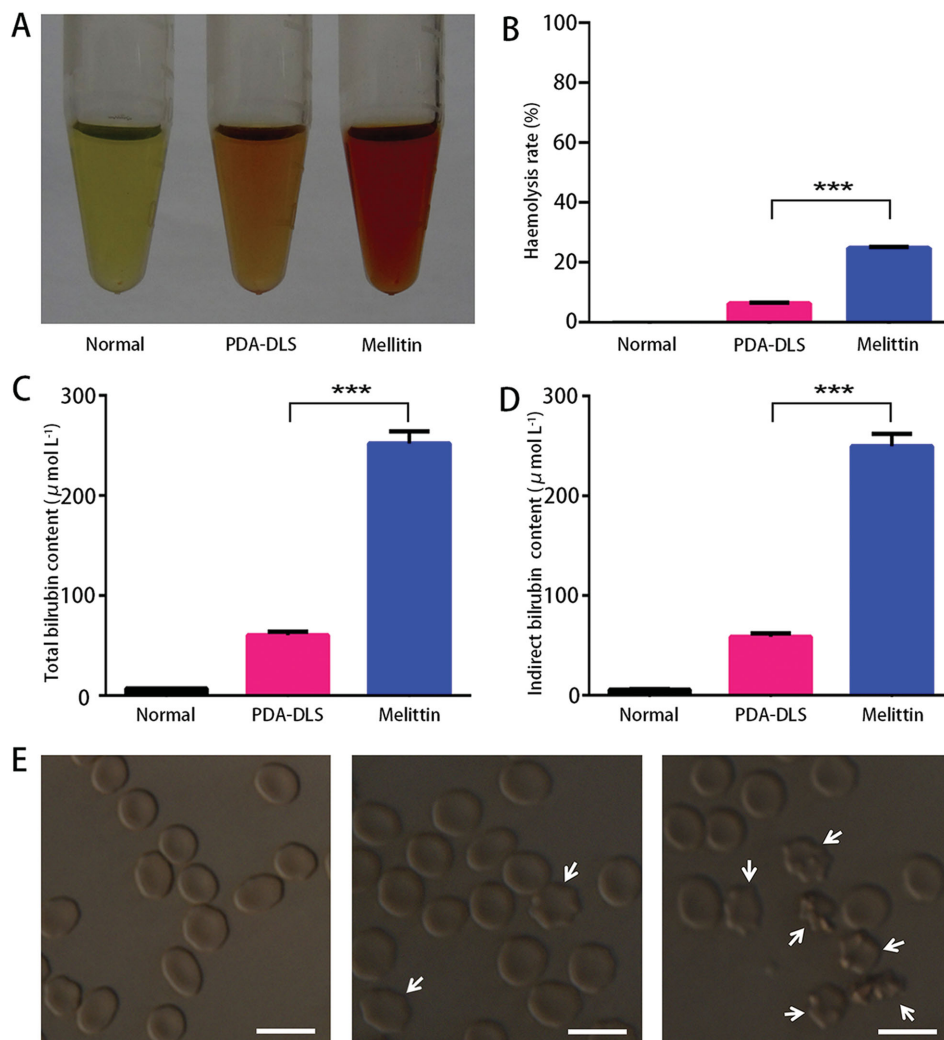
Figure 7. Cleansing human blood of PFTs by the PDA-DLS device. A) Centrifuged plasma of the melittin contaminated blood (10 µg mL^{-1}) treated by PDA-DLS device (PDA-DLS). The red color means the lysis of RBC. Normal human blood (Normal) and melittin contaminated human blood (10 µg mL^{-1}, Melittin) were used as the negative control and positive control, respectively. B) Hemolysis rate in Normal, PDA-DLS, and Melittin group. $n = 3$. C) Total bilrubin in Normal, PDA-DLS and Melittin group. $n = 3$. D) Indirect bilrubin in Normal, PDA-DLS and Melittin group. $n = 3$. E) Morphology of RBC in Normal (left), PDA-DLS (middle), and Melittin group (right). Ancanthocyte (arrow) is closely associated with hemolysis. Scale bars: 10 µm (E).

Inspired by liver-specific microstructure that facilitates hepatocytes to efficiently detoxify against toxins in the bloodstream, many attempts have been performed to prepare manmade liver-mimetic structures. However, it is very challenging for manufacture processes, like advanced 3D-printing, to reproduce such complex microarchitectures as a liver. Here, we used a decellularization technology to prepare a DLS that is mainly composed by collagens. The obtained DLS preserved the 3D architecture and hierarchical vasculature of a native liver. After the immobilization of nanoparticles, the DLS provided an ideal structure to facilitate nanoparticles to efficiently capture PFTs in bloodstream. Thus, our research revealed the promise of DLS in preparing advanced liver-mimetic devices.

Currently, recellularization is the only reported method to functionalize decellularized organ scaffolds including DLS for biomedical applications.[28–35] Because of using live cells, customization is always required for different patients, and it remains a challenge to harvest enough available cells in a short time. In this work, we used synthetic PDA nanoparticles that act like artificial hepatocytes to "recellularize" DLS, creating a bioinspired device with promising application in antidotal therapy. To our knowledge, this work is the first attempt to use synthetic nanoparticles to activate DLS to generate a functional medical device. This provides a new strategy to functionalize decellularized organ scaffolds for medical applications. Moreover, this strategy may allow the integration of a variety of functionalities and nanoelements in different acelluar organ scaffolds, and could lead to many breakthroughs in the development of future bio-inspired biomedical devices.

4. Conclusion

We described a method to functionalize DLS with nanoparticles, and constructed a liver-mimetic fluidic device that consists of a DLS populated by PDA nanoparticles. The
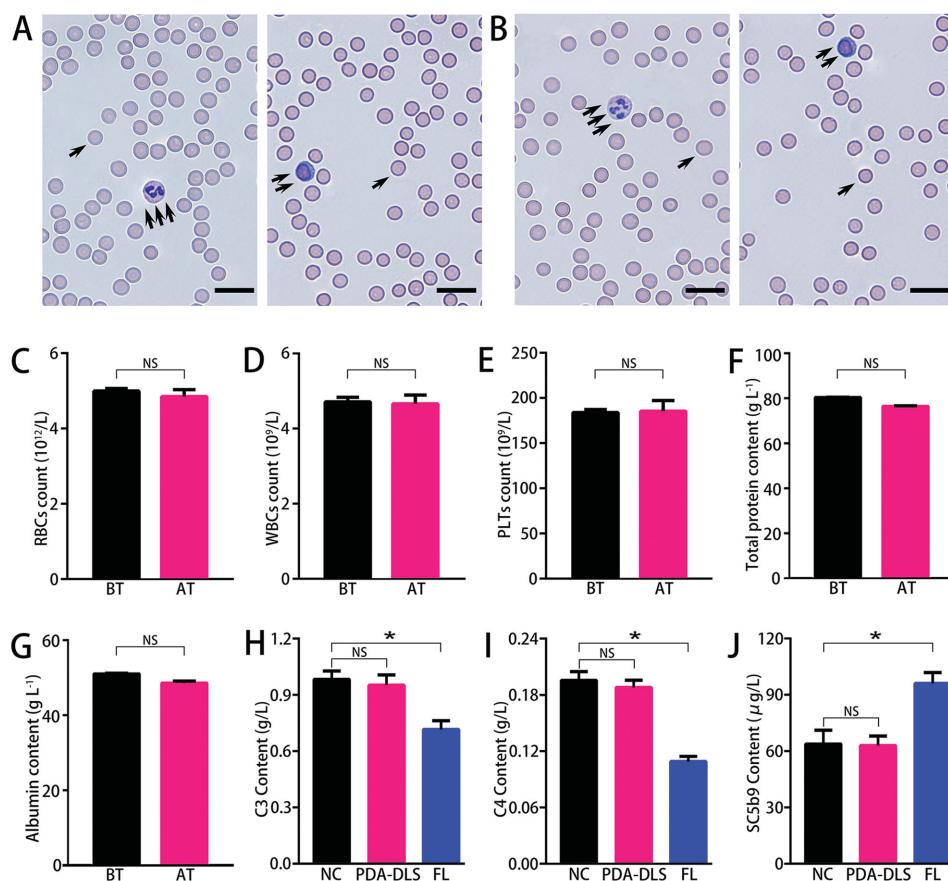
Figure 8. Safety assessment of the PDA-DLS device. A,B) Wright staining images of blood smears. Red blood cells (single arrow), lymphocytes (double arrow), and neutrophils (triple arrow) in normal human blood A) and the same human blood after perfusion through the PDA-DLS device (B). C) The number of red blood cells (RBC) before (BT) and after (AT) treated by the PDA-DLS device. $n = 3$. D) The number of white blood cells (WBCs) before (BT) and after (AT) treated by the PDA-DLS device. $n = 3$. E) The number of platelets (PLTs) before (BT) and after (AT) treated by the PDA-DLS diver. $n = 3$. F,G) Total protein (F) and albumin (G) in normal blood before (BT) and after (AT) treated by the PDA-DLS device. $n = 3$. H–J) C3 (H), C4 (I), and SC5b9 (J) in normal blood (normal control, NC), the PDA-DLS device treated blood (PDA-DLS) and the fresh liver treated blood (FL). $n = 3$. NS: no significant difference. Scale bars: 20 µm (A, B).

device could efficiently remove PFTs in blood, and would not significantly affect blood components and induce complement activation, showing promising applications in antidotal therapy against PFTs. This work provides a proof-of-principle of targeted blood detoxification by a nanoparticle-activated DLS, and could lead to many breakthroughs in the development of future detoxification devices.

5. Experimental Section

Preparation of DLS: The liver was retrieved from the upper abdomen of rats (Vital River Laboratories), and decellularized by a modified perfusion decellularization technique.[28] Male Sprague-Dawley rats (150–160 g) (Vital River Laboratories) were anesthetized with 1% Pelltobarbitalum Natricum (Sigma). The hepatic artery was ligated and 200 U of heparin was injected through cardiac puncture. The portal vein was clamped at the level of the inferior mesenteric vein and cannulated with an 18 G cannula (Harvard Apparatus). IVC was clamped at the level of the left renal vein and cannulated with a 22 G cannula (Harvard Apparatus). The liver was retrieved from the upper abdomen and connected with a perfusion

device to allow antegrade portal vein perfusion of heparinized PBS (Invitrogen) at 75 mm Hg portal vein pressure for 30 min to rid the residual blood. Then a decellularization solution was administered at 75 mm Hg of constant pressure in the following order: 12 h of 1% SDS (Sigma) in distilled water, 30 min of distilled water and 30 min of 1% TritonX-100 (Sigma) in distilled water. After decellularization, the liver was washed with distilled water for 3 h. All animal experiments were approved by the Institutional Animal Care and Use Committee of West China Hospital of Sichuan University.

Synthesis of PCDA-EDEA-SA-NHS: The synthesis scheme of PCDA-EDEA-SA-NHS has been presented in Figure. 4A. N-hydroxysuccinimideand (920 mg, 7.99 mmol) and 1-(3-Dimethylaminopropyl)-3-Ethylcarbodiimide (1020 mg, 5.32 mmol) were added into CH_2Cl_2 (100 mL) which contains compound 1 (10,12-pentacosadiynoic acid, 500 mg, 1.33 mmol) at room temperature. The reaction system was stirred at room temperature for 2 h to produce activated ester 2. Then the resulting solution was added into amine 4 (1980 mg, 13.35 mmol) drop by drop, stirred over night at room temperature. CH_2Cl_2 was removed from the resulting solution through vacuum distillation and the product was purified using silica gel column chromatography to obtain PCDA-EDEA. The solution system containing PCDA-EDEA (100 mg, 0.20 mmol) and

activated acid 3(230 mg, 1.95 mmol) was stirred over night at room temperature. The white solid end-product 5 (PCDA-EDEA-SA-NHS) was obtained after column purification. The yield was 15%.

Preparation of PDA Nanoparticles: The mixture containing PCDA (190 mg) and PCDA-EDEA-SA (10 mg) were added into hot water (100 mL, 70 °C), followed by probe sonication for 10 min. Then, the solution was stored at 4 °C overnight, and irradiated by UV at 254 nm for 10 min to produce blue PDA nanoparticles. When unmodified PDA nanoparticle was prepared, the PCDA-EDEA-SA was not applied.

Preparation of the PDA-DLS Device: To immobilize PDA nanoparticles in DLS, DLS was connected to an ALC-M Perfusion device (Shanghai Alcott Biotech CO.) via the portal vein cannulation. The IVC was left open for outlet. PDA nanoparticles (1 mg mL^{-1}, 50 mL) were pumped into DLS via the portal vein at 2 mL min^{-1}, and unmodified PDA nanoparticles were used as the control. This process was shown in the Supplementary video of the Supporting Information. The content of PDA nanoparticles in outflow was monitored by measuring the absorbance (A_E) of outflow at 640 nm. The absorbance of distilled water is A_0, while that of initial PDA solution is $A_{100\%}$. The adhesive rate was calculated by Equation (1)

$$\text{Adhesive rate (\%)} = 100 - (A_E - A_{0\%}) \times (A_{100\%} - A_{0\%})^{-1} \times 100 \tag{1}$$

To study the release of PDA nanoparticles from DLS, DLS reloaded with PDA nanoparticles was eluted with distilled water perfusion at 2 mL min^{-1} for 24 h. The content of released PDA nanoparticles from DLS was detected by measuring the absorbance (A_E) of the elutant at 640 nm. The absorbance of distilled water is A_0, while that of initial PDA solution is $A_{100\%}$. The content of PDA nanoparticles in the elutant and DLS was calculated by Equations (2) and (3), respectively,

$$\text{Content (\%)} = (A_E - A_{0\%}) \times (A_{100\%} - A_{0\%})^{-1} \times 100 \tag{2}$$

$$\text{Content (\%)} = 100 - (A_E - A_{0\%}) \times (A_{100\%} - A_{0\%})^{-1} \times 100 \tag{3}$$

The generated PDA-DLS device was then blocked by pumping glycine solution (10 g L^{-1}, 20 mL) at 2 mL min^{-1} for 10 min.

To further confirm PDA nanoparticles would not be released to circulating blood from PDA-DLS device, human fresh blood (50 mL) was circularly perfused through the device at 2 mL min^{-1}. After 20 min, 1 mL blood was taken out and then centrifuged at 800 g for 5 min. Controls consisted of human fresh blood (negative) and human fresh blood with 20 μg mL^{-1} PDA nanoparticles (positive), respectively. All supernatant plasma was collected and measured the absorbance (AE) at 640 nm. To quantify PDA nanoparticles in the supernatant plasma (Cp), a standard curve was simultaneously performed by measuring AE of a series of plasma with 0, 10, 20, 30, 40, 50 μg mL^{-1} PDA nanoparticles, respectively.

Detoxification Using the PDA-DLS Device: To assess the ability of PDA-DLS device to detoxify melittin, the PDA-DLS device and the fresh liver (as control) were processed into pieces with the volume of 100 mm^3, followed by incubation of each piece with melittin solutions (200 μL) of different concentrations. After incubation for 60 min at 37 °C, the samples were centrifuged, and the supernatants were added to rat RBCs' solution (4% v/v, 100 μL) and incubated for 30 min at 37 °C, separately. Samples were then centrifuged at 800 g for 5 min and the release of hemoglobin was measured by colorimetric reading. Controls for 0% and 100% neutralization of haemolytic activity consisted of RBCs incubated with 5 μg mL^{-1} melittin ($A_{0\%}$) and a RBC suspension with normal saline ($A_{100\%}$), respectively. The percentage of neutralization was calculated according to Equation (4):

$$\text{Neutralization(\%)} = 100 - (A_{sample} - A_{100\%}) \times (A_{0\%} - A_{100\%})^{-1} \times 100 \tag{4}$$

To detoxify the single-pass perfused melittin solution, the PDA-DLS device and DLS (as control) were connected to a perfusion device via portal vein cannulation. Melittin solution (10 μg mL^{-1}, 100 mL) was pumped into the PDA-DLS device or DLS through the portal vein at 2 mL min^{-1}, and flowed out from IVC to create a single-pass perfusion. In the process of perfusion, the outflow was collected every 5 min. Each outflow (100 μL) was added to RBCs' solution (4% v/v, 100 μL) for RBCs' lysis tests, and the detoxification efficiency was calculated using Equation (4).

To detoxify the circular perfused melittin solution, the PDA-DLS device was connected to the perfusion device via portal vein cannulation. Melittin solution (10 μg mL^{-1}, 100 mL) was pumped into the PDA-DLS device through the portal vein at 2 mL min^{-1}, and the outflow from IVC was collected by the melittin solution pool to create a circulation perfusion. The circulation lasted for 150 min. In the meantime, the melittin solution (100 μL) was taken out from the melittin solution pool every 25 min and added to the RBCs' solution (4% v/v, 100 μL) for RBCs' lysis tests. Then, the detoxification efficiency was calculated as Equation (4).

To detoxify melittin contaminated blood, the PDA-DLS device was connected to the perfusion device via portal vein cannulation. After mixing with melittin (10 μg mL^{-1}), the human blood (20 mL) from a healthy donator was pumped into the PDA-DLS device immediately at 2 mL min^{-1} for circular perfusion. The donor was aware of his blood use in our research and firmed a written consent, as from the declaration of Helsinki. The circulation continued for 20 min. Meanwhile, the same blood with or without melittin (10 μg mL^{-1}) served as Melittin group and Normal group to evaluate the quality of detoxified blood.

Analysis of the Impact of PDA-DLS Device on Normal Human Blood: The PDA-DLS device and the fresh liver (as control) were connected to the perfusion device via portal vein cannulation. The human blood (100 mL) from the healthy donor was pumped into the PDA-DLS device or the fresh liver at 2 mL min^{-1} for circulating perfusion. The donor was aware of his blood use in our research and firmed a written consent, as from the declaration of Helsinki. After circulating for 100 min, the blood was used for cellular morphology observation, complete blood count, blood biochemical analysis, and immune quantitation.

Determination of Collagen Content: DLS was cut into small pieces and put into centrifuge tubes. Then the samples were lyophilized and acid hydrolyzed with 6 M HCl at 105 °C for 12 h. The collagen content was measured indirectly through the measurement of hydroxyl proline content according to Jamall et al.[36]

Then the results were normalized to the weight of fresh liver (6.97 ± 0.21 g).

Histological Analysis: Fresh liver and DLS were frozen, and processed for staining with hematoxylin and eosin. Additional samples were incubated with rabbit polyclonal anti-collagen I, rabbit polyclonal anti-collagen IV, rabbit polyclonal anti-laminin β1, rabbit polyclonal anti-fibronectin, and rabbit polyclonal anti-elastin (Abcam). Secondary antibodies were anti-rabbit IgG PE conjugate (Santa Cruz). Counter staining was performed with DAPI (Sigma). Samples were imaged using Olympus BX51TF camera.

Scanning Electron Microscopy Imaging: DLS was fixed with 2% paraformaldehyde and 2.5% glutaraldehyde in 0.2 M sodium phosphate buffer at room temperature for 24 h. The fixed samples were washed three times with deionized water. The samples were dehydrated with a series of ethanol solutions of increasing concentration, 70%, 80%, 90%, and 100%. The samples were dried in Emitech K850X Critical Point Dryer and sputter coated with chromium. The samples were visualized using a JEOL 7500F field emission scanning electron microscope. To observe the location of PDA nanoparticles in the PDA-DLS device, the PDA-DLS device and DLS (as control) were fixed by liquid nitrogen flash freezing, and dried in Boyikang FD-1C-50 lyophilizer. The samples were then sputter coated with gold and visualized using a Hitachi S-4800 field emission scanning electron microscope.

Confocal Laser Scanning Microscope Imaging: After perfused with a melittin solution (10 µg mL^{-1}, 100 mL), the PDA-DLS device was processed to pieces with the size of $5 \times 3 \times 1$ mm. Then, the samples were sealed with nonfluorescence mounting agent in concave slide, and underwent 3D imaging using a Nikon A1R confocal laser scanning microscope.

Supporting Information

Supporting Information is available from the Wiley Online Library or from the author.

Acknowledgements

[1] J. H. Kang, M. Super, C. W. Yung, R. M. Cooper, K. Domansky, A. R. Graveline, T. Mammoto, J. B. Berthet, H. Tobin, M. J. Cartwright, A. L. Watters, M. Rottman, A. Waterhouse, A. Mammoto, N. Gamini, M. J. Rodas, A. Kole, A. Jiang, T. M. Valentin, A. Diaz, K. Takahashi, D. E. Ingber, *Nat. Med.* **2014**, *20*, 1211.

[2] M. Gou, X. Qu, W. Zhu, M. Xiang, J. Yang, K. Zhang, Y. Wei, S. Chen, *Nat. Commun.* **2014**, *5*, 3774.

[3] B. Struecker, N. Raschzok, I. M. Sauer, *Nat. Rev. Gastroenterol. Hepatol.* **2014**, *11*, 166.

[4] M. W. Parker, S. C. Feil, *Prog. Biophys. Mol. Biol.* **2005**, *88*, 91.

[5] M. Michalek, F. D. Sönnichsen, R. Wechselberger, A. J. Dingley, C. Hung, A. Kopp, H. Wienk, M. Simanski, R. Herbst, I. Lorenzen, F. Marciano-Cabral, C. Gelhaus, T. Gutsmann, A. Tholey, J. Grötzinger, M. Leippe, *Nat. Chem. Biol.* **2013**, *9*, 37.

[6] F. C. Los, T. M. Randis, R. V. Aroian, A. J. Ratner, *Microbiol. Mol. Biol. Rev.* **2013**, *77*, 173.

[7] B. S. Gold, R. C. Dart, R. A. Barish, *N. Engl. J. Med.* **2002**, *347*, 1804.

[8] C. E. Dempsey, *Biochim. Biophys. Acta.* **1990**, *1031*, 143.

[9] H. Bayley, *Nature* **2009**, *459*, 651.

[10] K. Yoshimatsu, H. Koide, Y. Hoshino, K. J. Shea, *Nat. Protoc.* **2015**, *10*, 595.

[11] V. Forster, J. C. Leroux, *Sci. Transl. Med.* **2015**, *7*, 290ps14.

[12] Y. Liu, J. Du, M. Yan, M. Y. Lau, J. Hu, H. Han, O. O. Yang, S. Liang, W. Wei, H. Wang, J. Li, X. Zhu, L. Shi, W. Chen, C. Ji, Y. Lu, *Nat. Nanotechnol.* **2013**, *8*, 187.

[13] Y. Hoshino, H. Koide, K. Furuya, W. W. Haberaecker, S. H. Lee, T. Kodama, H. Kanazawa, N. Oku, K. J. Shea, *Proc. Natl. Acad. Sci. USA* **2012**, *109*, 33.

[14] L. M. Graham, T. M. Nguyen, S. B. Lee, *Nanomedicine (London, U. K.)* **2011**, *6*, 921.

[15] J. C. Leroux, *Nat. Nanotechnol.* **2007**, *2*, 679.

[16] C. M. Hu, R. H. Fang, J. Copp, B. T. Luk, L. Zhang, *Nat. Nanotechnol.* **2013**, *8*, 336.

[17] C. M. Hu, R. H. Fang, B. T. Luk, L. Zhang, *Nat. Nanotechnol.* **2013**, *8*, 933.

[18] B. Struecker, N. Raschzok, I. M. Sauer, *Nat. Rev. Gastroenterol. Hepatol.* **2014**, *11*, 166.

[19] D. E. Malarkey, K. Johnson, L. Ryan, G. Boorman, R. R. Maronpot, *Toxicol. Pathol.* **2005**, *33*, 27.

[20] Y. Lu, Y. Yang, A. Sellinger, M. Lu, J. Huang, H. Fan, R. Haddad, G. Lopez, A. R. Burns, D. Y. Sasaki, J. Shelnutt, C. J. Brinker, *Nature* **2001**, *410*, 913.

[21] J. Lee, H. T. Chang, H. An, S. Ahn, J. Shim, J. M. Kim, *Nat. Commun.* **2013**, *4*, 2461.

[22] X. Wang, X. Sun, P. Hu, J. Zhang, L. Wang, W. Feng, S. Lei, B. Yang, W. Cao, *Adv. Funct. Mater.* **2013**, *23*, 6044.

[23] H. Peng, X. Sun, F. Cai, X. Chen, Y. Zhu, G. Liao, D. Chen, Q. Li, Y. Lu, Y. Zhu, Q. Jia, *Nat. Nanotechnol.* **2009**, *4*, 738.

[24] X. Chen, G. Zhou, X. Peng, J. Yoon, *Chem. Soc. Rev.* **2012**, *41*, 4610.

[25] O. Yarimaga, J. Jaworski, B. Yoon, J. M. Kim, *Chem. Commun.* **2012**, *48*, 2469.

[26] R. Jelinek, M. Ritenberg, *RSC Adv.* **2013**, *3*, 21192.

[27] A. Nel, T. Xia, L. Madler, N. Li, *Science* **2006**, *311*, 622.

[28] B. E. Uygun, A. Soto-Gutierrez, H. Yagi, M. L. Izamis, M. A. Guzzardi, C. Shulman, J. Milwid, N. Kobayashi, A. Tilles, F. Berthiaume, M. Hertl, Y. Nahmias, M. L. Yarmush, K. Uygun, *Nat. Med.* **2010**, *16*, 814.

[29] S. F. Badylak, D. Taylor, K. Uygun, *Annu. Rev. Biomed. Eng.* **2011**, *13*, 27.

[30] J. E. Arenas-Herrera, I. K. Ko, A. Atala, J. J. Yoo, *Biomed. Mater.* **2013**, *8*, 014106.

[31] H. C. Ott, T. S. Matthiesen, S. K. Goh, L. D. Black, S. M. Kren, T. I. Netoff, D. A. Taylor, *Nat. Med.* **2008**, *14*, 213.

[32] T. H. Petersen, E. A. Calle, L. Zhao, E. J. Lee, L. Gui, M. B. Raredon, K. Gavrilov, Z. Yi, Z. W. Zhuang, C. Breuer, E. Herzog, L. E. Niklason, *Science* **2010**, *329*, 538.

[33] H. C. Ott, B. Clippinger, C. Conrad, C. Schuetz, I. Pomerantseva, L. Ikonomou, D. Kotton, J. P. Vacanti, *Nat. Med.* **2010**, *16*, 927.

[34] J. J. Song, J. P. Guyette, S. E. Gilpin, G. Gonzalez, J. P. Vacanti, H. C. Ott, *Nat. Med.* **2013**, *19*, 646.

[35] P. Macchiarini, P. Jungebluth, T. Go, M. A. Asnaghi, L. E. Rees, T. A. Cogan, A. Dodson, J. Martorell, S. Bellini, P. P. Parnigotto, S. C. Dickinson, A. P. Hollander, S. Mantero, M. T. Conconi, M. A. Birchall, *Lancet* **2008**, *372*, 2023.

[36] I. S. Jamall, V. N. Finelli, S. S. Que Hee, *Anal. Biochem.* **1981**, *112*, 70.